Proteostasis collapse is a driver of cell aging and death

Mantu Santra[a,b,1], Ken A. Dill[a,c,d,2], and Adam M. R. de Graff[a,e,1]

[a]Laufer Center for Physical and Quantitative Biology, Stony Brook University, Stony Brook, NY 11794-5252; [b]Department of Chemical, Biological & Macro-Molecular Sciences, S. N. Bose National Centre for Basic Sciences, Kolkata-700106, India; [c]Department of Physics and Astronomy, Stony Brook University, Stony Brook, NY 11794-3800; [d]Department of Chemistry, Stony Brook University, Stony Brook, NY 11794-3400; and [e]Babraham Research Campus, Methuselah Health UK Ltd., Cambridge, United Kingdom CB22 3AT

Contributed by Ken A. Dill, September 13, 2019 (sent for review April 17, 2019; reviewed by Uri Alon and Anat Ben-Zvi)

What molecular processes drive cell aging and death? Here, we model how proteostasis—i.e., the folding, chaperoning, and maintenance of protein function—collapses with age from slowed translation and cumulative oxidative damage. Irreparably damaged proteins accumulate with age, increasingly distracting the chaperones from folding the healthy proteins the cell needs. The tipping point to death occurs when replenishing good proteins no longer keeps up with depletion from misfolding, aggregation, and damage. The model agrees with experiments in the worm *Caenorhabditis elegans* that show the following: Life span shortens nonlinearly with increased temperature or added oxidant concentration, and life span increases in mutants having more chaperones or proteasomes. It predicts observed increases in cellular oxidative damage with age and provides a mechanism for the Gompertz-like rise in mortality observed in humans and other organisms. Overall, the model shows how the instability of proteins sets the rate at which damage accumulates with age and upends a cell's normal proteostasis balance.

proteostasis | aging | oxidative damage | misfolding | chaperones

In higher organisms, cells age and die by natural processes. What are the molecular mechanisms that drive it? It has been difficult to disentangle causes from effects because aging impacts most cellular biomolecules. Oxidative damage is known to play a key role. Much of what is known about cellular aging comes from "bottom-up" experiments, by perturbing a few genes at a time—by knockouts, knock-ins, or point mutations or by gene-to-gene comparisons using sequence databases (1). Our interest here is in the "top-down" question of the aging mechanism, which we take to be a more system-wide failure in the cell. Any single gene cannot reverse aging or abolish life span limits. Oxidative damage is indiscriminate and nonspecific in which class of biomolecule it hits or its spatial location in the cell. We take the mechanism of aging and longevity to be more about a general and stochastic destruction than a pinpoint action.

Theories of cell aging are diverse (1–5). Some theories are gene-centric, attributing primary importance to deleterious changes to DNA that accumulate throughout life (6). Such changes include mutations (7) and the progressive shortening of telomeres (8, 9). Other theories are epigenetic, focusing on how changes to DNA and DNA-binding proteins affect how genes are read. These changes include DNA methylation, histone modification, and loss of chromosomal organization (1). Further, the significant depletion of histone levels and changes in their stoichiometry (10) could alter transcription factor binding (11). Such changes may be responsible for the loss of proper messenger RNA and protein stoichiometry observed with age (12–16).

Another view is that aging results from declining protein quality-control systems involved in protein synthesis, degradation, and chaperoning that normally protect the proteins in the cell's proteome (17–20). Central to proteostasis, the decline in protein quality control is implicated in more than 50 diseases of abnormal protein deposition (proteinopathies), for which the principal risk factor is advancing age, "probably because cell regulation and protein production and disposal becomes increasingly compromised with age" (21). Proteostasis is a natural culprit in aging because it is a front line of response to stress and because proteins are the primary repairers of the cell and sustainers of the genome (10). It has been noted that "all known gerontogenes confer resistance to stress" (22). Protein damage is a key measure of such resistance, as survival of radiation is better predicted by protein oxidation than by DNA damage (23, 24). Damage to proteins can lead to loss of their stability and function (25–27) and to impaired protein synthesis (24) and degradation (28). While protein damage is only one of a broad set of changes impacting the proteome with age (15, 29), it is an important component. We focus not on the genetics and biochemistry of any particular gene or protein, but on the cell-wide biophysics of how proteins fold (30), the impact of temperature and oxidation (25, 31), and how proteostasis declines with age.

Previous models of proteostasis have focused primarily on the mechanism of heat-shock activation (20, 32) or the means by which chaperone systems promote folding (33–35). Others have looked for broader principles determining folding yield (36) or partitioning between folding and degradation (37). While these studies have contributed to a solid understanding of protein properties upstream of damage, their downstream properties and impact remain poorly studied (20, 32). Our modeling addresses the critical impact of protein conformation on oxidizability (38–40) and the role of damaged protein in diverting

Significance

Cells and organisms grow old and die. We develop a biophysical model of the mechanism. Young cells are kept healthy by the positive processes of protein synthesis, degradation, and chaperoning (the activity of keeping proteins properly folded). But, with age, negative processes increase: Oxidative damage accumulates randomly in the cell's proteins, healthy synthesis and degradation slow down, and—like overfilled garbage cans—chaperone capacity is exceeded. The chaperones are distracted trying to fold irreversibly damaged proteins, leading to accumulating misfolded and aggregated proteins in the cell. The tipping point to death happens when the negative overwhelms the positive. The model makes several quantitative predictions of the life span of the worm *Caenorhabditis elegans*.

Author contributions: M.S., K.A.D., and A.M.R.d.G. designed research; M.S. and A.M.R.d.G. performed research; M.S. and A.M.R.d.G. analyzed data; and M.S., K.A.D., and A.M.R.d.G. wrote the paper.

Reviewers: U.A., Weizmann Institute; and A.B.-Z., Ben-Gurion University of the Negev.

The authors declare no competing interest.

[1]M.S. and A.M.R.d.G. contributed equally to this work.

[2]To whom correspondence may be addressed. Email: dill@laufercenter.org.

This article contains supporting information online at www.pnas.org/lookup/suppl/doi:10.1073/pnas.1906592116/-/DCSupplemental.

First published October 16, 2019.

the limited chaperone resources away from the folding of their undamaged counterparts (40, 41).

Premises of the Proteostasis Collapse Model

Here is our model of proteostasis collapse with age. The mathematical details, parameters, and justifications are given in *Materials and Methods* and *SI Appendix*. First, each protein in the cell has a rate of folding, unfolding, misfolding, and aggregation. Many of these rates are known (33, 43, 44). Here, we considered a single type of average protein—namely, ones that are clients of the HSP70 chaperone system, because of experiments (45) and theory (40) showing that these proteins are the dominant targets of protein oxidation. Second, we modeled the trafficking of proteins on and off of chaperones. Many of these rates, too, are known (46–49). Third, whereas these first 2 aspects—folding and chaperone trafficking—describe only normal proteostasis in young healthy cells, we included also a slow, cumulative oxidative-damage component that is known for cell growth and protein degradation (50, 51). Some of this damage will be irreversible, leading to proteins that cannot reach their functional native structures and thus are biased toward misfolding and aggregation. Of necessity, we leave out many details, such as the folding of membrane proteins, the mitochondrial generation of energy, and regulatory processes. It is not our goal to model everything. Here are the premises:

1) Each protein in a cell has an intrinsic propensity to fold or misfold. Most proteins carry out their function only when in their properly folded, native conformation (17–19). Here, we model the folding process of an average HSP70 chaperone-dependent protein as it transitions between 4 conformational states: its folded, functional native state (N), unfolded state (U), misfolded state (M), and aggregated state (A) (Fig. 1). The interconversion processes are modeled by using coupled Ordinary Differential Equations (ODEs) (*Materials and Methods* and *SI Appendix*). The transition rates and equilibria between these states were previously determined (33, 40, 42), as well as their dependencies on temperature (*SI Appendix*).
2) Each protein sustains damage at a rate determined by its foldedness. A principal cause of proteome aging is oxidative damage (27, 52). Both experimental (38, 39) and theoretical (40) studies support the idea that nonnative conformations are the major target of oxidative damage. As in previous work (40), the flux of damage $J_{dam} = k_{dam}[U]$, where k_{dam} is the rate constant of damage, scaling proportionately to reactive oxygen species (ROS) levels, and [U] is the concentration of unfolded protein (see *SI Appendix*, Table S1 for parameter values). Once oxidized, proteins are assumed to be unable to fold, as shown in Fig. 1, consistent with experiments (45).
3) Chaperones modulate the foldedness and damage levels of their client proteins. Chaperones are proteins that help other proteins (their clients) fold. By binding to nonnative conformations and giving them a fast route to folding, ATP-dependent chaperones are responsible for maintaining a high degree of foldedness (53). The collective effect of these chaperones, called foldases, is modeled by taking the kinetics and concentrations of their dominant member, the HSP70 chaperones (12) (*SI Appendix*). Given that nonnative conformations are thought to be the major target of oxidation, chaperones play a key role in controlling damage levels (40, 45).
4) Chaperones can become preoccupied handling damaged proteins that are unable to fold, preventing them from helping their undamaged client proteins that are either newly synthesized or spontaneously unfolded (54–56). Experimental support for this assumption includes the increased chaperone binding observed for proteins with disease-causing point mutations, which mirror the destabilizing effects of side-chain oxidation (25, 57, 58). Further, the presence of oxygen (and hence ROS) has been shown to significantly amplify the heat-shock response during the periods of high mistranslation, a process evoked when chaperones become titrated (45). Due to the inability of irreversibly damaged proteins to fold, their repeated binding to chaperones creates a futile cycle that can only be terminated by their degradation or aggregation.
5) Proteome health also depends on the rates of synthesis and degradation of proteins. To complete the model, we therefore need to know how the rates of cell growth $k_{gr}(t)$ and degradation $k_{deg}(t)$ change with age, t. Given the highly regulated nature of these processes, it is outside the scope of the current model to predict them from first principles. Instead, since both have been measured experimentally (12, 50) (*SI Appendix*, Fig. S1), we take them as inputs to the model, approximating the data using exponential fits: $k_{gr} = k_{gr}^{o} e^{-\lambda_{gr} t}$ and $k_{deg} = k_{deg}^{o} e^{-\lambda_{deg} t}$, where k_{gr}^{o} and k_{deg}^{o} are the initial values. The decay constants are determined from fitting the experimental data, giving values at 20 °C of $\lambda_{gr} = 0.4$ d^{-1} and $\lambda_{deg} = 0.14$ d^{-1}, respectively. These rates are assumed to scale with temperature following Arrhenius kinetics, doubling roughly every 8 °C, as observed for enzymatic processes (*SI Appendix*, Eq. **S4** and Table S1).

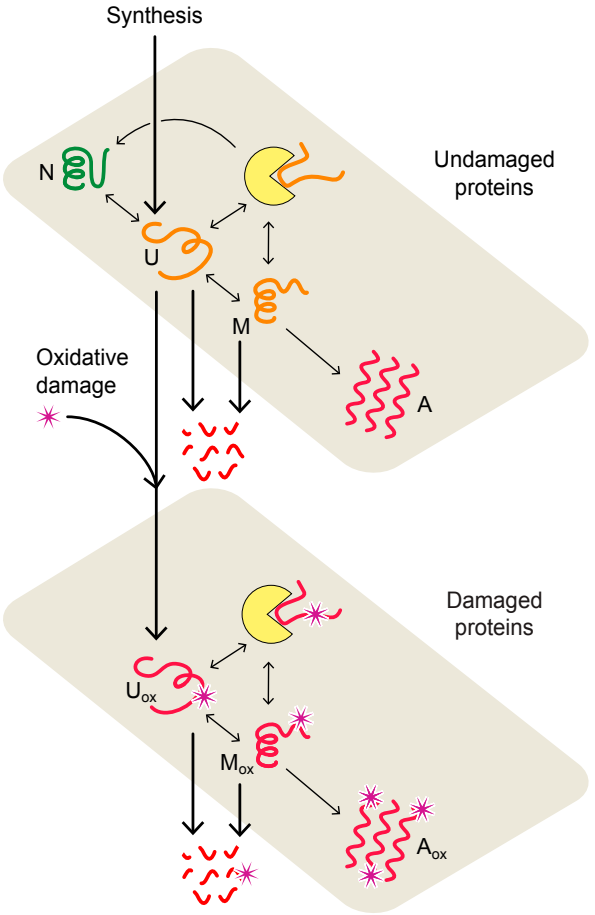

Fig. 1. Proteostasis model of cell aging. In the model, proteins convert between native (N), unfolded (U), misfolded (M), and aggregated (A) states (upper plane) with rates estimated from experimental data (33, 42). Chaperone-dependent folding of newly synthesized or thermally unfolded proteins compete with the processes of protein oxidation, aggregation, and degradation, collectively defining the quality of the proteome and proteostasis at a given age. The lower plane describes the interconversion of oxidatively damaged unfolded (U_{ox}), misfolded (M_{ox}), and aggregated (A_{ox}) states. Chaperones are represented by yellow disks.

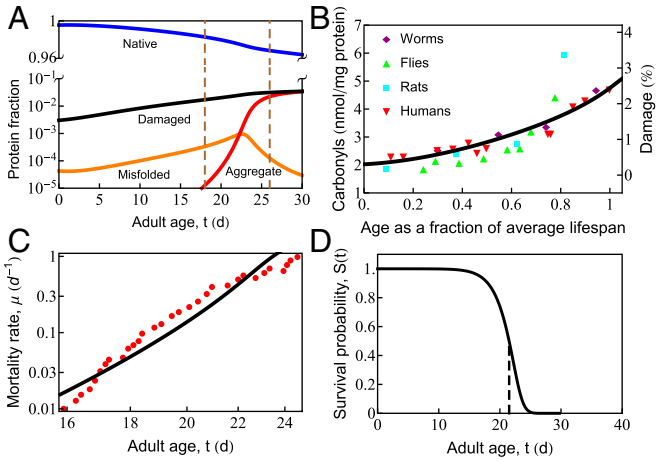

Fig. 2. In cell aging, oxidative damage leads to increased misfolding and aggregation, which eventually causes cell death. (*A*) The age-dependent slowing of synthesis and degradation causes the accumulation of damaged (black line), misfolded (orange line), and aggregated (red line) states and depletion of the native (blue line) state. Progressive cell aging causes proteostasis to transition through 2 phases: 1) the progressive titration of chaperones by damaged proteins, causing the accumulation of misfolded protein, followed by 2) misfolded proteins crossing their solubility threshold, triggering late-life aggregation (the region inside the vertical dashed lines). (*B*) The gradual increase of protein damage with age in different organisms, as measured by carbonyl content. The black line indicates the percentage of damaged protein predicted by the current model. (*C*) Age-dependent mortality rate data at $T = 20.1$ °C (red symbols). The black line is the theoretical fit to the data. (*D*) Predicted survival curve in wild-type *Caenorhabditis elegans* at $T = 20$ °C. The vertical dashed line shows the point of 50% survival and is taken as the average life span of the organism.

By solving the ODEs (*SI Appendix* and *Materials and Methods*) with the parameters described above, we can compute how the rates of trafficking, folding, and aggregation of an average HSP70 chaperone client protein changes over time as oxidative damage accumulates. Below, we show the resulting predictions for several properties—the survival probability $S(t)$ reflecting the fraction of the population remaining alive at time t; the corresponding mortality rate $\mu = -d(lnS)/dt$ describing the death rate per individual; the distribution of protein between folded, misfolded, aggregated, and damaged states; and their dependence on temperature or added oxidizing agent—and compare them to corresponding experiments in the worm. The model gives a picture of how proteostasis collapse contributes to cell aging and death.

How Does Proteostasis Decline with Age?

Misfolding and Aggregation Grow Nonlinearly with Age. Fig. 2*A* shows predicted properties as a function of age. Healthy proteostasis in young cells (the first few days in the worm) is achieved by the dilution of damaged proteins due to the high rates of growth. However, fast growth is short-lived, with protein synthesis rates declining 10-fold over the reproductive time window (12). As the synthesis of new protein slows with age, the production of healthy protein no longer keeps up with the rate of oxidative damage, causing damage levels to rise (Fig. 2 *A* and *B*). Rising damage results in increased misfolding of the proteome (Fig. 2*A*, orange curve), as chaperones become increasingly preoccupied in futile attempts to refold irreversibly damaged proteins. This leaves fewer chaperones to fold the healthy undamaged proteins the cell needs to function. As misfolded proteins approach their solubility limit, the concentration of aggregates increases exponentially (Fig. 2*A*, red curve) before reaching a plateau. This predicted sequence of events is consistent with experiments, which find: 1) an exponential rise in damage levels (Fig. 2*B*) (25, 27); 2) increased protein misfolding (59); and, finally, 3) the rapid onset of aggregation that appears to grow exponentially (60) before reaching a plateau (12). The model is also qualitatively consistent with the observed Gompertzian, time-dependent mortality rate and associated survival probability (Fig. 2 *C* and *D*), although it does lack late-life slowing in mortality seen experimentally (61, 62) and modeled elsewhere (62). For discussion of the mortality rate $\mu(t)$ and survival probability $S(t)$, see *SI Appendix*.

How Does Life Span Depend on Environmental Properties?

Life Span Shortens with Increasing Temperature. In simple organisms, life span has a remarkable and strong dependence on temperature (51, 61). Maintained at higher temperatures, organismal life span shortens considerably. For example, *Caenorhabditis elegans* grown at 20 °C lives about 22 d, yet at 25 °C, they live only 10 d (61). Qualitatively, such observations appear to support the Rate-of-Living Hypothesis (63)—namely, that life span is shorter at higher temperatures because of faster metabolism, which, in turn, is expected from the physical chemistry of Arrhenius kinetics dictating the temperature-dependent acceleration of biochemical reactions (64, 65). In that theory, the rate of aging is proportional to the speed of these reactions, so a plot of the logarithm of the inverse life span (which is a rate of living) vs. $1/T$ (T is the absolute temperature) should give a straight line with a slope equal to the activation energy of the process. However, Fig. 3*C* shows that life span follows a more complex behavior

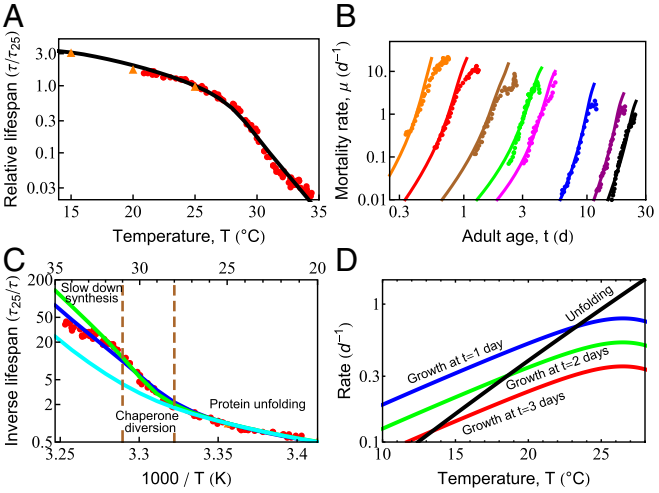

Fig. 3. Temperature dependence of survival probability and life span is dictated by the fundamental properties of proteins. (*A*) Predicted decay of life span with increasing temperature (black line), compared with experimental data from Stroustrup et al. (61) (red circles) and Van Voorhies and Ward (51) (orange triangles). (*B*) Predicted rates of mortality at different temperatures (solid lines) compared with experimental data from Stroustrup et al. (61) (symbols). The temperatures are, from black to orange, 20 °C (20.1 °C), 22.1 °C (23.7 °C), 25.5 °C (25.2 °C), 28.3 °C (29.1 °C), 28.9 °C (30 °C), 30 °C (30.9 °C), 31.3 °C (31.3 °C), and 32.4 °C (32.5 °C); the values in the brackets are those reported in Stroustrup et al. (61). (*C*) The inverse life span as a function of inverse absolute temperature shows distinct regions in which different processes dominate life-span behavior. The blue line represents the prediction of the current model. The green line is the prediction in the absence of the slowed growth rate observed experimentally at high temperatures (*SI Appendix*, Fig. S2, orange line). The cyan curve represents the prediction if damaged proteins are not allowed to bind and effectively deplete chaperones. (*D*) With increasing temperature, the average unfolding rate of proteins (black line) increases faster than enzymatic processes like protein synthesis, shown at 1, 2, and 3 d of adulthood (blue, green, and red lines, respectively).

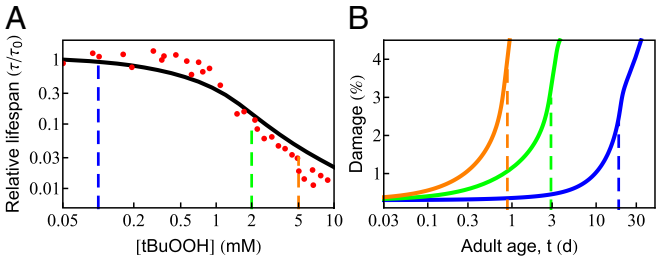

Fig. 4. Effect of oxidative damage on survival probability and life span. (*A*) The predicted dependence of life span on the concentration of external oxidant, tBuOOH (black solid line), compared with experimental data [red circles; Stroustrup et al. (61)]. Beyond a critical concentration (0.5 mM), life span drops sharply in an approximately power-law fashion. (*B*) The age-dependent rise in protein damage is shown for 3 concentrations of tBuOOH (indicated by vertical dashed lines in *A*). The vertical dashed lines in *B* indicate the average life span.

than the Rate-of-Living Hypothesis would predict. Our model gives the following interpretation.

Heating at normal temperatures between 15 °C and 24 °C increases metabolism. Across the proteome, and across species, enzymatic rates are known to roughly double for every 8 °C rise in temperature, following Arrhenius kinetics (*SI Appendix*, Eq. **S4**). Around room temperature, the dominant proteostasis processes—synthesis, folding, degradation, and their rates of decay—all scale similarly with temperature, causing life span to scale inversely with metabolic rate. Thus, over this narrow temperature range, life span scales consistently with the Rate-of-Living Hypothesis (63).

At Temperatures from 24 °C to 28 °C, Protein Unfolding Rates Begin to Exceed Synthesis Rates. Protein unfolding rates have a steeper temperature dependence than other proteostasis processes, roughly doubling every 4 °C (66, 67). By using kinetics inferred previously for HSP70 clients (33), unfolding rates are predicted to catch up to the rates of protein synthesis in early adulthood within this temperature range (Fig. 3*D*). This rapid acceleration of spontaneous unfolding of proteins is a central reason why greater chaperone levels are beneficial at higher temperatures, regulated through the heat-shock response (68). Yet, oddly, this stress response is turned off very early in *C. elegans* adulthood (69). Other stress-response pathways such as the mitochondrial unfolded protein response and the endoplasmic reticulum unfolded protein response are also strongly down-regulated (59) by a mechanism that can be modulated by gonadal signaling (70–72) and dietary restriction (73). Given that a single temperature was used to raise the worms (61), our model therefore uses a single, constant chaperone level for all adult temperature conditions and ages (12).

Heating at Temperatures Above 28 °C Rapidly Fills Available Chaperone Capacity, Forcing Protein Synthesis to Slow. Life span is predicted to shorten much more rapidly at temperatures above 28 °C, as unfolding loads begin to overshadow synthesis (*SI Appendix, Effective Parameters*). The temperature dependence of the total unfolding burden faced by the cell thus transitions from a synthesis-dominated regime, where the burden doubles every 8 °C, to an unfolding-dominated regime, where the burden doubles every 4 °C. At such high unfolding loads, we hypothesized that life span might be particularly sensitive to the burden from damaged proteins. To test this, we modeled aging with (blue) and without (cyan) the ability for damaged proteins to bind chaperones. Consistent with our hypothesis, chaperone distraction by damaged proteins begins decreasing life span between T = 28 °C and 31 °C (Fig. 3*C*). This sensitivity is further compounded by the rising levels of unfolded, oxidation-prone proteins at these temperatures. Together, these processes provide a dangerous feedback loop that may explain why the heat-shock response is highly sensitive to the presence of damaging free radicals (41).

The increasing diversion of chaperones away from the folding of newly synthesized proteins may also be why, above 28 °C, an additional behavior is observed experimentally: Growth begins to slow (*SI Appendix*, Fig. S2). In this extreme heat, slowing growth may be one of the few mechanisms the cell has to diminish the folding burden and delay proteostasis collapse. To test this, we modeled aging with (blue) and without (green) slowed growth (Fig. 3*C*). The difference between the 2 curves suggests that slower synthesis provides a modest benefit to life span, predicted to make a 2-fold difference by $T = 35$ °C. It reiterates a key result observed throughout our modeling—namely, that proteostasis capacity is tightly coupled to the rate of protein synthesis.

In short, while our model does show a component of life span that is attributable to the rate-of-living via metabolic speed-up, it also shows an additional component based on cell stresses. As the cell is stressed by heat, proteins unfold, misfold, and aggregate. Chaperones are recruited, but with age, the synthesis of "good protein" and the chaperoning of those spontaneously unfolding ultimately succumb to damage levels, at which bad protein becomes overwhelming.

Life Span Shortens with Added Oxidant Concentration. Since oxidation is a well-known aging agent, adding an oxidant to cells should decrease their life span, as shown in recent experiments (61). To explore the behavior predicted from the proteostasis model, we assumed that damage to the proteome occurs in linear proportion to the amount of oxidant, consisting of the basal level of ROS made by the cell as well as that from the added oxidant *tert*-butyl hydroperoxide (tBuOOH). The damage rate can be expressed as $k_{dam} = k^o_{dam}(1 + \frac{[tBuOOH]}{c_o})$, where k^o_{dam} is the rate of damage in the absence of tBuOOH and c_o is a constant with units of concentration, determined by the best fit to experimental data. Fig. 4*A* shows that the predicted life span (black curve) agrees well with the experimental measurements [red points; Stroustrup et al. (61)]. Life span changes very little at low levels of tBuOOH, as it makes only a small contribution to the overall damage rate. However, beyond a critical value, life span drops sharply. The age-dependent rise in protein damage is shown in Fig. 4*B* for 3 values of [tBuOOH] (shown by vertical dashed lines in Fig. 4*A*). Consistent with the experimental observation, the extent of damage at death (Fig. 4*B*, vertical dashed lines) increases with shortening life span (74, 75).

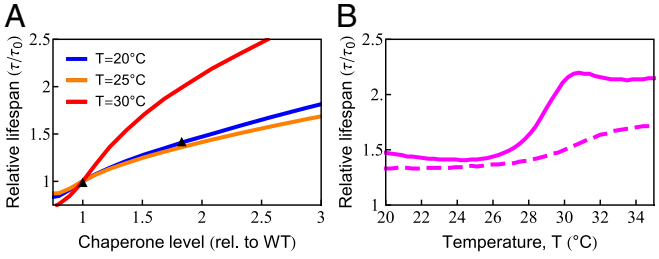

Fig. 5. Increased chaperone capacity extends life span. (*A*) Chaperone dependence of relative (rel.) life span (τ/τ_o, where τ_o is the life span with wild-type [WT] chaperone level) at $T = 20$ °C (blue line), $T = 25$ °C (orange line), and $T = 30$ °C (red line). The predicted increase of life span (orange line) quantitatively captures the experimentally observed life span extension at $T = 25$ °C (black triangles) (77). (*B*) The temperature dependence of life-span extension due to a 2-fold increase in chaperone level with (solid line) and without (dashed line) the ability of chaperones to bind, and thus be titrated by, damaged protein.

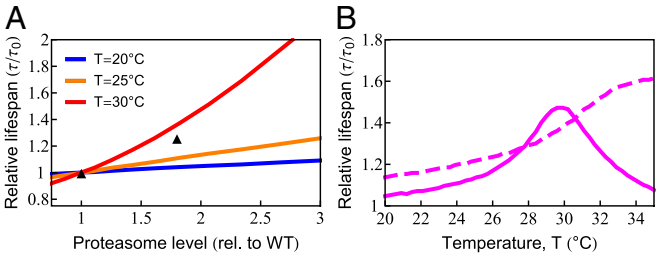

Fig. 6. Increased degradation capacity extends life span. (*A*) Increasing degradation capacity is predicted to increase life span at different temperatures. The black symbols are experimental data at $T = 20$ °C. (83). rel., relative; WT, wild type. (*B*) The benefit of increased degradation capacity depends highly on temperature (solid line). The dashed line is the model prediction in the absence of chaperone diversion.

How Does Life Span Depend on Cellular Properties?

Chaperone Overexpression Can Extend Life Span. The model gives an accounting for how chaperone levels can affect a cell's aging and longevity. Chaperones reduce the levels of unfolded, oxidation-prone conformations, thereby decreasing the rates of protein damage and aggregation (76). Proteins are susceptible to damage when they are synthesized, as well as during each thermal unfolding event, which occurs in our model at a rate $k_u \approx 0.4$ d^{-1} at $T = 20$ °C (*SI Appendix*, Table S1). To explore this dependence more precisely, we predicted life span for chaperone levels ranging from 80 to 300% of the wild-type value at 3 different temperatures, as shown in Fig. 5*A*. The model predicts that at $T = 25$ °C, an 80% increase in chaperone level can increase life span by ≈45%. This is in quantitative agreement with the experimental observation (77). Extension of life span by increasing chaperone levels has also been observed in other studies on *C. elegans* (78, 79), fruit flies (80), and mice (81). Although there are apparent exceptions, such as the acceleration of neurodegeneration upon overexpression of HSP90 in mice (82), it should be noted that HSP90 can be a negative regulator of the HSP70 chaperones studied here. Interestingly, life-span extension from increased chaperone availability is predicted to have a strong nonlinear temperature dependence, rising sharply above 28 °C (Fig. 5*B*, solid line), coincident with the sharp rise in chaperone diversion and the inhibition of protein synthesis observed experimentally (*SI Appendix*, Fig. S2). To test if damaged proteins play a central role in this model behavior, we turned off the ability of damaged proteins to bind chaperones. When we did, the strong nonlinear behavior largely disappeared (Fig. 5*B*, dashed line). As chaperones cannot be strongly upregulated in adult worms (69), Fig. 5*B* shows the importance of freeing up chaperone capacity by decreasing synthesis at high temperatures.

Overexpressing the Degradation Machinery Extends Life Span. The model also predicts the dependence of cellular life span on degradation rates. Proteasome overexpression has been shown to extend life span by directly ridding the cell of protein damage and indirectly by controlling the levels of regulatory proteins (83). By up-regulating degradation capacity in the model, we found—similar to chaperones—that life span can be extended significantly (83) (Fig. 6*A*). The amount of benefit also showed nonmonotonic behavior due to chaperone diversion by damaged proteins (Fig. 6*B*). Consistent with these predictions, upregulating 26S proteasomal activity showed negligible benefits at 20 °C, yet increased life span by 25% at 25 °C (71). However, experiments showed continued life-span benefit at 34 °C, where death normally occurs in less than a day, suggesting that our model may not be adequately capturing certain processes under such severe stress conditions.

Conclusions. We describe how proteostasis declines with age in the worm *C. elegans*. The model explains 2 remarkable experimental results from ref. 61—namely, that worms' life span decreases by 2 orders of magnitude when they are grown in heat or added oxidant. Most importantly, the model gives an underlying mechanistic explanation for how this dependence emerges from well-known properties of protein-folding kinetics and the targeting of nonnative protein conformations by oxidants. This, in turn, provides a mechanism for one of the most prominent features of aging—namely, the nonlinear increase in death rate with age, called Gompertz Law. With age, the abundances of irreparably damaged proteins are predicted to increase, distracting the chaperones from folding the healthy proteins the cell needs. The tipping point to death occurs when replenishing good proteins no longer keeps up with losses from damage and aggregation. The progressive aging of the proteome is seen to be a direct consequence of slowed protein synthesis and turnover, relative to the relentless onslaught of damage.

Materials and Methods

To run the model, a numerical differential equation solver in Mathematica was applied to the equations describing the folding, misfolding, chaperoning, damage, aggregation, or degradation of protein (*SI Appendix*). Growth rate k_{gr} was initialized at 20 °C by using values in *SI Appendix*, Table S1. Protein concentration was held constant by using the following relation between synthesis [$\sigma(t)$], growth [$k_{gr}(t)$], and degradation flux [$J_{deg}(t)$], $\sigma(t) = k_{gr}(t)[P] + J_{deg}(t)$, where [$P$] is the desired total concentration of the protein. The concentration of chaperone was kept constant over time (*SI Appendix*, Table S1). Prior to allowing the system to age ($t > 0$), the system was equilibrated at $T = 20$ °C for long enough (10 d) to make sure that the system reached steady state, as indicated by the time independence of concentrations of proteins, chaperones, and chaperone-bound complexes. At this point, corresponding to the starting point of *C. elegans* adulthood, we imposed the age-dependent decay of growth and degradation (*SI Appendix*, Table S1). The simulation was carried out for a further 1 d, keeping temperature fixed at 20 °C in the absence of external oxidative stress. After the end of this day, we imposed the change corresponding to the stress of interest (temperature, oxidative damage, chaperone level, or proteasome level) by changing the associated parameters in *SI Appendix*, Table S1. Following the experimental convention of Stroustrup et al. (61), we defined this time as $t = 0$.

The current model predicts damage level with increasing age. The damage level is generally considered as a biomarker of aging. To predict the mortality rate, we assumed that it was proportional to the damage level following the relation: $\mu(t) = \mu_o f_D(t)^\alpha$, where $f_D(t)$ is the fraction of damaged protein, and μ_o and α are constants which are obtained by fitting the experimental data shown in Fig. 2*C* (see *SI Appendix* for further details).

ACKNOWLEDGMENTS. This work was supported by the Laufer Center for Physical and Quantitative Biology and by NSF Grant PHY1205881. We thank Dr. Meng-Qiu Dong for her valuable insight that helped initiate this work; Dr. Sarina Bromberg for assistance with figures; and the reviewers for their helpful comments.

1. C. Lopez-Otin, M. Blasco, L. Partridge, M. Serrano, G. Kroemer, The hallmarks of aging. *Cell* **153**, 1194–1217 (2013).
2. T. Kirkwood, Understanding the odd science of aging. *Cell* **120**, 437–447 (2005).
3. A. Kowald, T. Kirkwood, A network theory of ageing: The interactions of defective mitochondria, aberrant proteins, free radicals and scavengers in the ageing process. *Mutat. Res.* **316**, 209–236 (1996).
4. C. Soti, P. Csermely, Aging and molecular chaperones. *Exp. Gerontol.* **38**, 1037–1040 (2003).
5. J. McAuley, R. Taylor, A. Simonds, S. Chawda, Respiratory difficulty with palatal, laryngeal and respiratory muscle tremor in adult-onset Alexander's disease. *BMJ Case Rep.*, 10.1136/bcr-2016-218484 (2017).
6. J. Hoeijmakers, DNA damage, aging, and cancer. *N. Engl. J. Med.* **361**, 1475–1485 (2009).
7. R. Bahar *et al.*, Increased cell-to-cell variation in gene expression in ageing mouse heart. *Nature* **441**, 1011–1014 (2006).
8. E. Blackburn, C. Greider, J. Szostak, Telomeres and telomerase: The path from maize, *Tetrahymena* and yeast to human cancer and aging. *Nat. Med.* **12**, 1133–1138 (2006).

9. B. Jesus *et al.*, Telomerase gene therapy in adult and old mice delays aging and increases longevity without increasing cancer. *EMBO Mol. Med.* **4**, 691–704 (2012).
10. J. Feser *et al.*, Elevated histone expression promotes life span extension. *Mol. Cell* **39**, 724–735 (2010).
11. Y. Field *et al.*, Distinct modes of regulation by chromatin encoded through nucleosome positioning signals. *PLoS Comput. Biol.* **4**, e1000216 (2008).
12. D. Walther *et al.*, Widespread proteome remodeling and aggregation in aging *C. elegans*. *Cell* **161**, 919–932 (2015).
13. R. Houtkooper *et al.*, Mitonuclear protein imbalance as a conserved longevity mechanism. *Nature* **497**, 451–457 (2013).
14. G. Janssens *et al.*, Protein biogenesis machinery is a driver of replicative aging in yeast. *eLife* **4**, e08527 (2015).
15. S. Rangaraju *et al.*, Suppression of transcriptional drift extends *C. elegans* lifespan by postponing the onset of mortality. *eLife* **4**, e08833 (2015).
16. V. Narayan *et al.*, Deep proteome analysis identifies age-related processes in *C. elegans*. *Cell Systems* **3**, 144–159 (2016).
17. W. Balch, R. I. Morimoto, A. Dillin, J. Kelly, Adapting proteostasis for disease intervention. *Science* **319**, 916–919 (2008).
18. E. Powers, R. Morimoto, A. Dillin, J. Kelly, W. Balch, Biological and chemical approaches to diseases of proteostasis deficiency. *Annu. Rev. Biochem.* **78**, 959–991 (2009).
19. R. Taylor, A. Dillin, Aging as an event of proteostasis collapse. *Cold Spring Harbor Perspect. Biol.* **3**, a004440 (2011).
20. C. Proctor, I. Lorimer, Modelling the role of the Hsp70/Hsp90 system in the maintenance of protein homeostasis. *PLoS One* **6**, e22038 (2011).
21. L. Walker, H. LeVine III, Corruption and spread of pathogenic proteins in neurodegenerative diseases. *J. Biol. Chem.* **287**, 33109–33115 (2012).
22. J. Vanfleteren, B. Braeckman, Mechanisms of life span determination in *Caenorhabditis elegans*. *Neurobiol. Aging* **20**, 487–502 (1999).
23. A. Krisko, M. Radman, Protein damage and death by radiation in *Escherichia coli* and *Deinococcus radiodurans*. *Proc. Natl. Acad. Sci. U.S.A.* **107**, 14373–14377 (2010).
24. A. Krisko, M. Radman, Phenotypic and genetic consequences of protein damage. *PLoS Genet.* **9**, e1003810 (2013).
25. A. de Graff, M. Hazoglou, K. Dill, Highly charged proteins: The Achilles' heel of aging proteomes. *Structure* **24**, 329–336 (2016).
26. D. Petrov, B. Zagrovic, Microscopic analysis of protein oxidative damage: Effect of carbonylation on structure, dynamics, and aggregability of villin headpiece. *J. Am. Chem. Soc.* **133**, 7016–7024 (2011).
27. E. Stadtman, Protein oxidation and aging. *Science* **257**, 1220–1224 (1992).
28. N. Sitte *et al.*, Proteasome inhibition by lipofuscin/ceroid during postmitotic aging of fibroblasts. *FASEB J.* **14**, 1490–1498 (2000).
29. D. L. Hatfield, Redox pioneer: Professor Vadim N. Gladyshev. *Antioxid. Redox Signaling* **25**, 1–9 (2016).
30. K. Ghosh, A. de Graff, L. Sawle, K. Dill, Role of proteome physical chemistry in cell behavior. *J. Phys. Chem. B* **120**, 9549–9563 (2016).
31. L. Sawle, K. Ghosh, How do thermophilic proteins and proteomes withstand high temperature? *Biophys. J.* **101**, 217–227 (2011).
32. C. J. Proctor *et al.*, Modelling the actions of chaperones and their role in ageing. *Mech. Ageing Dev.*. **126**, 119–131 (2005).
33. M. Santra, D. Farrell, K. Dill, Bacterial proteostasis balances energy and chaperone utilization efficiently. *Proc. Natl. Acad. Sci. U.S.A.* **114**, E2654–E2661 (2017).
34. E. T. Powers, D. L. Powers, L. M. Gierasch, FoldEco: A model for proteostasis in *E. coli*. *Cell Rep.* **1**, 265–276 (2012).
35. K. Chen *et al.*, Thermosensitivity of growth is determined by chaperone-mediated proteome reallocation. *Proc. Natl. Acad. Sci. U.S.A.* **114**, 11548–11553 (2017).
36. S. Chakrabarti, C. Hyeon, X. Ye, G. H. Lorimer, D. Thirumalai, Molecular chaperones maximize the native state yield on biological times by driving substrates out of equilibrium. *Proc. Natl. Acad. Sci. U.S.A.* **114**, E10919–E10927 (2017).
37. S. Bershtein, W. Mu, A. W. Serohijos, J. Zhou, E. I. Shakhnovich, Protein quality control acts on folding intermediates to shape the effects of mutations on organismal fitness. *Mol. Cell* **49**, 133–144 (2013).
38. M. Girod *et al.*, Structural basis of protein oxidation resistance: A lysozyme study. *PLoS One* **9**, e101642 (2014).
39. A. Vidovic, F. Supek, A. Nikolic, A. Krisko, Signatures of conformational stability and oxidation resistance in proteomes of pathogenic bacteria. *Cell Rep.* **7**, 1393–1400 (2014).
40. M. Santra, K. Dill, A. de Graff, How do chaperones protect a cell's proteins from oxidative damage? *Cell Systems* **6**, 743–751 (2018).
41. A. Fredriksson, M. Ballesteros, S. Dukan, T. Nystrom, Induction of the heat shock regulon in response to increased mistranslation requires oxidative modification of the malformed proteins. *Mol. Microbiol.* **59**, 350–359 (2006).
42. M. Kerner *et al.*, Proteome-wide analysis of chaperonin-dependent protein folding in *Escherichia coli*. *Cell* **122**, 209–220 (2005).
43. K. Ghosh, K. A. Dill, Computing protein stabilities from their chain lengths. *Proc. Natl. Acad. Sci. U.S.A.* **106**, 10649–10654 (2009).
44. G. C. Rollins, K. A. Dill, General mechanism of two-state protein folding kinetics. *J. Am. Chem. Soc.* **136**, 11420–11427 (2014).
45. A. Fredriksson, M. Ballesteros, S. Dukan, T. Nystrom, Defense against protein carbonylation by Dnak/Dnaj and proteases of the heat shock regulon. *J. Bacteriol.* **187**, 4207–4213 (2005).
46. J. Hohfeld, Y. Minami, F. U. Hartl, Hip, a novel cochaperone involved in the eukaryotic Hsc70/Hsp40 reaction cycle. *Cell* **83**, 589–598 (1995).
47. J. Hohfeld, S. Jentsch, GrpE-like regulation of the hsc70 chaperone by the anti-apoptotic protein BAG-1. *EMBO J.* **16**, 6209–6216 (1997).
48. D. Bimston *et al.*, BAG-1, a negative regulator of hsp70 chaperone activity, uncouples nucleotide hydrolysis from substrate release. *EMBO J.* **17**, 6871–6878 (1998).
49. L. Sun *et al.*, The lid domain of *Caenorhabditis elegans* Hsc70 influences ATP turnover, cofactor binding and protein folding activity. *PLoS One* **7**, e33980 (2012).
50. G. Depuydt, N. Shanmugam, M. Rasulova, I. Dhondt, B. P. Braeckman, Increased protein stability and decreased protein turnover in the *Caenorhabditis elegans* ins/IGF-1 daf-2 mutant. *J. Gerontol. Ser.A* **71**, 1553–1559 (2016).
51. W. Van Voorhies, S. Ward, Genetic and environmental conditions that increase longevity in *Caenorhabditis elegans* decrease metabolic rate. *Proc. Natl. Acad. Sci. U.S.A.* **96**, 11399–11403 (1999).
52. M. Radman, Protein damage, radiation sensitivity and aging. *DNA Repair* **44**, 186–192 (2016).
53. N. B. Nillegoda, A. S. Wentink, B. Bukau, Protein disaggregation in multicellular organisms. *Trends Biochem. Sci.*. **43**, 285–300 (2018).
54. S. Kim, E. A. Nollen, K. Kitagawa, V. P. Bindokas, R. I. Morimoto, Polyglutamine protein aggregates are dynamic. *Nat. Cell Biol.* **4**, 826–831 (2002).
55. T. Gidalevitz, A. Ben-Zvi, K. H. Ho, H. R. Brignull, R. I. Morimoto, Progressive disruption of cellular protein folding in models of polyglutamine diseases. *Science* **311**, 1471–1474 (2006).
56. A. Yu *et al.*, Protein aggregation can inhibit clathrin-mediated endocytosis by chaperone competition. *Proc. Natl. Acad. Sci. U.S.A.* **111**, E1481–E1490 (2014).
57. G. Karras *et al.*, Hsp90 shapes the consequences of human genetic variation. *Cell* **168**, 856–866 (2017).
58. N. Tokuriki, F. Stricher, J. Schymkowitz, L. Serrano, D. Tawfik, The stability effects of protein mutations appear to be universally distributed. *J. Mol. Biol.* **369**, 1318–1332 (2007).
59. A. Ben-Zvi, E. Miller, R. Morimoto, Collapse of proteostasis represents an early molecular event in *Caenorhabditis elegans* aging. *Proc. Natl. Acad. Sci. U.S.A.* **106**, 14914–14919 (2009).
60. D. David *et al.*, Widespread protein aggregation as an inherent part of aging in *C. elegans*. *PLoS Biol.* **8**, e1000450 (2010).
61. N. Stroustrup *et al.*, The temporal scaling of *Caenorhabditis elegans* ageing. *Nature* **530**, 103–107 (2016).
62. O. Karin, A. Agrawal, Z. Porat, V. Krizhanovsky, U. Alon, Senescent cells and the dynamics of aging. bioRxiv (13 April 2019).
63. R. Pearl, *The Rate of Living* (University of London Press Ltd., London, U.K., 1928).
64. H. Suda, K. Sato, Y. Shimizu, A further test of the equation of lifespan by *C. elegans*: Effective activation energy for aging and lifespan. *Exp. Gerontol.* **46**, 569–578 (2011).
65. H. Suda, K. Sato, S. Yanase, Timing mechanism and effective activation energy concerned with aging and lifespan in the long-lived and thermosensory mutants of *Caenorhabditis elegans*. *Mech. Ageing Dev.* **133**, 600–610 (2012).
66. M. Guo, Y. Xu, M. Gruebele, Temperature dependence of protein folding kinetics in living cells. *Proc. Natl. Acad. Sci. U.S.A.* **109**, 17863–17867 (2012).
67. M. Holtzer *et al.*, Temperature dependence of the folding and unfolding kinetics of the GCN4 leucine zipper via 13C-NMR. *Biophys. J.* **80**, 939–951 (2001).
68. S. Lindquist, The heat-shock response. *Ann. Rev. Biochem.* **55**, 1151–1191 (1986).
69. J. Labbadia, R. Morimoto, Repression of the heat shock response is a programmed event at the onset of reproduction. *Mol. Cell* **59**, 639–650 (2015).
70. N. Shemesh, N. Shai, A. Ben-Zvi, Germline stem cell arrest inhibits the collapse of somatic proteostasis early in *Caenorhabditis elegans* adulthood. *Aging Cell* **12**, 814–822 (2013).
71. D. Vilchez *et al.*, RPN-6 determines *C. elegans* longevity under proteotoxic stress conditions. *Nature* **489**, 263–270 (2012).
72. L. R. Lapierre, A. Meléndez, M. Hansen, Autophagy links lipid metabolism to longevity in *C. elegans*. *Autophagy* **8**, 144–146 (2012).
73. N. Shpigel, N. Shemesh, M. Kishner, A. Ben-Zvi, Dietary restriction and gonadal signaling differentially regulate post-development quality control functions in *Caenorhabditis elegans*. *Aging Cell* **18**, e12891 (2019).
74. H. Adachi, Y. Fujiwara, N. Ishii, Effects of oxygen on protein carbonyl and aging in *Caenorhabditis elegans* mutants with long (age-1) and short (mev-1) life spans. *J. Gerontol. Ser. A* **53A**, B240–B244 (1998).
75. K. Yasuda, H. Adachi, Y. Fujiwara, N. Ishii, Protein carbonyl accumulation in aging Dauer formation-defective (daj) mutants of *Caenorhabditis elegans*. *J. Gerontol. Ser. A* **54A**, 847–851 (1999).
76. H. H. Kampinga, S. Bergink, Heat shock proteins as potential targets for protective strategies in neurodegeneration. *Lancet Neurol.* **15**, 748–759 (2016).
77. K. Yokoyama *et al.*, Extended longevity of Caenorhabditis elegans by knocking in extra copies of hsp70F, a homolog of mot-2 (mortalin)/mthsp70/Grp75. *FEBS Lett.* **516**, 53–57 (2002).
78. A. L. Hsu, C. T. Murphy, C. Kenyon, Regulation of aging and age-related disease by DAF-16 and heat-shock factor. *Science* **300**, 1142–1145 (2003).
79. J. F. Morley, R. I. Morimoto, Regulation of longevity in *Caenorhabditis elegans* by heat shock factor and molecular chaperones. *Mol. Biol. Cell* **15**, 657–664 (2004).
80. G. Morrow, M. Samson, S. Michaud, R. Tanguay, Overexpression of the small mitochondrial Hsp22 extends *Drosophila* life span and increases resistance to oxidative stress. *FASEB J.* **18**, 598–599 (2017).
81. N. V. Bobkova *et al.*, Exogenous Hsp70 delays senescence and improves cognitive function in aging mice. *Proc. Natl. Acad. Sci. U.S.A.* **112**, 16006–16011 (2015).
82. L. Blair *et al.*, Accelerated neurodegeneration through chaperone-mediated oligomerization of tau. *J. Clin. Investig.* **123**, 4158–4169 (2013).
83. N. Chondrogianni, K. Georgila, K. Kourtis, N. Tavernarakis, E. Gonos, 20S proteasome activation promotes life span extension and resistance to proteotoxicity in *Caenorhabditis elegans*. *FASEB J.* **29**, 611–622 (2015).